



CHORUS

This is the accepted manuscript made available via CHORUS. The article has been published as:

Magneto-optical effects in semimetallic $\text{Bi}_{1-x}\text{Sb}_x$ ($x=0.015$)

S. V. Dordevic, M. S. Wolf, N. Stojilovic, M. V. Nikolic, S. S. Vujatovic, P. M. Nikolic, and L. C. Tung

Phys. Rev. B **86**, 115119 — Published 12 September 2012

DOI: [10.1103/PhysRevB.86.115119](https://doi.org/10.1103/PhysRevB.86.115119)

Magneto-optical effects in semi-metallic $\text{Bi}_{1-x}\text{Sb}_x$ with $x = 0.015$

S.V. Dordevic* and M.S. Wolf

Department of Physics, The University of Akron, Akron, Ohio 44325, USA

N. Stojilovic

Department of Physics and Astronomy, University of Wisconsin Oshkosh, Oshkosh, Wisconsin 54901, USA

M.V. Nikolic

Institute for Multidisciplinary Research, University of Belgrade, Kneza Visaslava 1, 11000 Belgrade, Serbia

S.S. Vujatovic and P.M. Nikolic

Serbian Academy of Sciences and Arts, 11000 Belgrade, Serbia

L.C. Tung

National High Magnetic Field Laboratory, Tallahassee, Florida, 32310, USA and

Department of Physics and Astronomy, University of North Dakota, Grand Forks, North Dakota, 58202, USA

(Dated: August 28, 2012)

We report the results of infrared and magneto-optical spectroscopy study on electrodynamic response of bismuth doped with 1.5 % of antimony. The spectra are presented for temperatures down to 4.2 K, and in magnetic fields as high as 18 Tesla. The results reveal strong magneto-optical activity, similar to pure bismuth, however there are some differences introduced by antimony doping. Analysis of optical functions reveals that the two type of charge carriers respond differently to external magnetic field. Finally, when the system enters the extreme quantum regime, both the inter- and intra-band Landau Level transition are observed in the spectra.

PACS numbers: 78.20.Ci, 78.30.-j, 74.25.Gz

I. INTRODUCTION

Elemental bismuth and its alloys with antimony $\text{Bi}_{1-x}\text{Sb}_x$ are subject of renewed interested in recent years due to realization of novel topological insulating (TI) state^{1,2}. $\text{Bi}_{1-x}\text{Sb}_x$ has been predicted theoretically and shown experimentally to be the first 3D topological insulator^{1,2}. Namely, as semi-metallic Bi is doped with Sb its semi-metallic character is suppressed; its band structure gradually evolves caused by strong spin-orbit coupling, and TI regime is archived for doping levels $0.07 < x < 0.22$ ^{1,2}. This novel 3D TI state is currently at the focus of interests for its unusual properties, especially in bulk materials like $\text{Bi}_{1-x}\text{Sb}_x$, Bi_2Se_3 , etc. Indeed, $\text{Bi}_{1-x}\text{Sb}_x$ has been shown experimentally using Angle Resolved Photo-Emission Spectroscopy (ARPES) to exhibit linear electron dispersions in the form of Dirac cones on its surface^{3,4}. Moreover, these Dirac electrons are topologically protected from scattering on non-magnetic impurities^{1,2,5}.

Infrared (IR) spectroscopy has been an indispensable experimental tool in studies of systems with correlated electrons, as it provides insight into electrodynamic properties inaccessible by other experimental techniques⁶⁻⁸. In this paper we present our results on the far-infrared and magneto-optical properties of $\text{Bi}_{1-x}\text{Sb}_x$ with $x=0.015$. At this doping the material is still in the semi-metallic regime, however our results reveal that the properties of bismuth have been significantly altered even with 1.5 % of antimony.

II. EXPERIMENTAL RESULTS

The samples for this study were grown at the Serbian Academy of Sciences and Arts using Bridgman method⁹. Initial materials (Bi and Sb) of very high purity level (6N) were kept in vacuumized quartz ampule. The content of the ampule was melted at approximately 800 °C, and then kept at 650 °C for 72 hours. The ampule was then gradually lowered into a cold zone, at approximately 2 mm/h. The product was a monocrystal ingot, which was then cut into cylindrically shaped samples for optical measurements. Before the measurements, the samples were mechanically polished, to achieve optically flat surface.

Zero magnetic field far-infrared measurements were performed at The University of Akron, at several selected temperatures between 10 and 300 K. An overcoating technique, with gold or aluminum coating of the sample as reference, was used to obtain the absolute values of reflectance¹⁰. Magneto-optical measurements were done at the National High Magnetic Field Laboratory for magnetic fields up to 18 Tesla, where the reflectance ratios $R(B)/R(0 \text{ Tesla})$ were measured. The absolute values of reflectance in magnetic field $R(B)$ was obtained as the product of the ratios with the absolute values of reflectance in zero field¹¹.

Figure 1(a) shows the far-infrared reflectance at several selected temperatures between 4.2 K and room temperature. The plasma minimum is located at 275 cm^{-1} at 300 K, and as temperature decreases it shifts to 170 cm^{-1} at

200 K, but stays at approximately the same frequency down to 4.2 K. We were able to obtain very good fits to the data in the far-IR frequency range using a simple Drude model⁶⁻⁸:

$$\varepsilon(\omega) = \varepsilon_\infty + \sum_i \frac{\omega_{p,i}^2}{-\omega^2 - i\gamma_i\omega} \quad (1)$$

where ε_∞ is the high frequency dielectric constant. To achieve satisfactory fits, two Drude modes ($i = 1,2$) were necessary, but with different plasma frequencies ω_p and scattering rates γ . We phenomenologically assign these two Drude modes to two different types of charge carriers. Indeed, Bi and $\text{Bi}_{1-x}\text{Sb}_x$ have long been known to have both electrons and holes present¹², albeit with densities much smaller than in typical metals. From the fits we also learn that as temperature decreases, the plasma frequencies $\omega_{p,1}$ and $\omega_{p,2}$ of both Drude-like modes (i.e. both type of carriers) are increasing, whereas the scattering rates γ_1 and γ_2 are decreasing.

In the zero-field reflectance spectra we note several similarities, but also several differences compared with pure Bi¹³. At room temperature the plasma minimum is slightly lower than in pure Bi, but the value of reflectance at the minimum is similarly high in both cases (about 50 %). As temperature decreases, the plasma edge in reflectance of pure Bi gradually shifts to lower frequencies down to lowest temperatures. On the other hand in $\text{Bi}_{1-x}\text{Sb}_x$ the plasma minimum is essentially temperature independent below 200 K. We also note that the so-called plasmaron peak^{13,14}, labeled as mode α by LaForge et al.¹³, is completely suppressed in $\text{Bi}_{1-x}\text{Sb}_x$, even at 4.2 K. In pure Bi on the other hand, the plasmaron peak appears at frequencies slightly above the plasma minimum¹³.

Figure 1(b) displays the absolute values of reflectance of $\text{Bi}_{1-x}\text{Sb}_x$ at several selected magnetic field values between 0 and 18 Tesla. The effect of magnetic field on the optical properties is strong and most prominent around the plasma minimum. As magnetic field increases, the plasma edge is suppressed and a characteristic "second plasma edge" gradually develops. We label this mode as γ , following the notation of LaForge et al.¹³. At the lowest frequencies and at the highest magnetic fields, the reflectance displays characteristic downturn, labeled as mode δ . These effects of magnetic field are similar to that in pure bismuth¹³. Note however that, similar to mode α , mode β is also absent from the spectra of $\text{Bi}_{1-x}\text{Sb}_x$, as compared with pure Bi¹³.

III. DISCUSSION

Since Kramers-Kronig analysis is not applicable to IR data in magnetic field, we resort to fitting. The simplest, but most frequently used model is the Drude-Lorentz model modified for the presence of magnetic field¹⁵. In

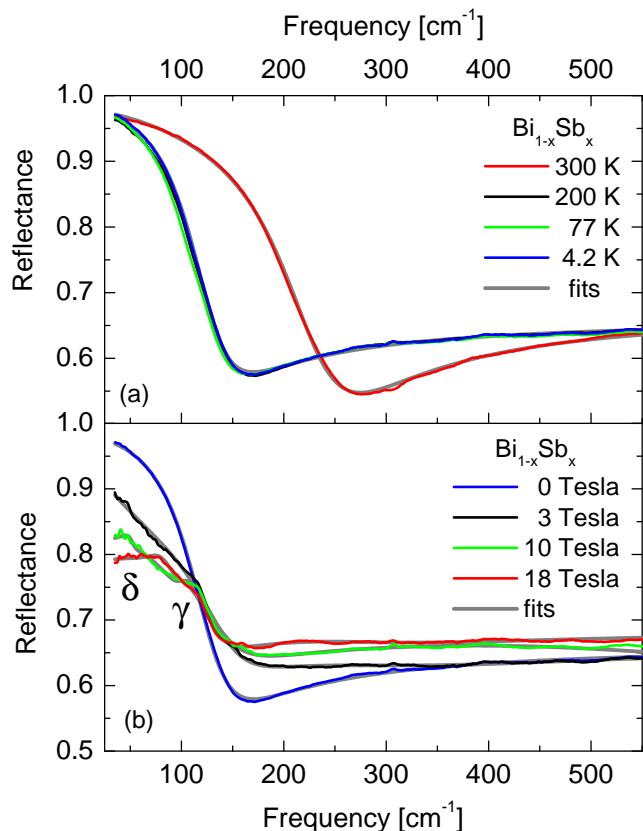


FIG. 1: (Color online). (a) Reflectance spectra of $\text{Bi}_{1-x}\text{Sb}_x$ with $x = 0.015$ in zero magnetic field at several different temperatures. The plasma edge moves dramatically between 300 and 200 K, but remains almost unchanged below 200 K. Also shown with gray lines are Drude fits (Eq. 1) of reflectance at 5 and 300 K. (b) Reflectance spectra of $\text{Bi}_{1-x}\text{Sb}_x$ at 4.2 K and at several magnetic fields up to 18 Tesla. The effect of magnetic field is similar to that on elemental bismuth: the original plasma edge is suppressed both below and above the plasma minimum. In addition, a second plasma edge develops around 100 cm⁻¹. Also shown with gray lines are the fits obtained from Eq. 2.

this model, components of the dielectric function tensor $\varepsilon_{\pm}(\omega) = \varepsilon_{xx} \pm i\varepsilon_{xy}$ are given as:

$$\varepsilon_{\pm}(\omega) = \varepsilon_\infty + \sum_i \frac{\omega_{p,i}^2}{\omega_{0,i}^2 - \omega^2 - i\gamma_i\omega \mp \omega_{c,i}\omega} \quad (2)$$

where ω_c is the cyclotron frequency, which can be both positive and negative depending on the type of charge carriers. This is particularly important for $\text{Bi}_{1-x}\text{Sb}_x$, where both electron- and hole-like carriers are known to be present. Another advantage of this model is that Eq. 2 reduces to Eq. 1 for $\omega_0 = 0$ and $\omega_c = 0$. In addition, this model allows both free ($\omega_0 = 0$) and bound ($\omega_0 \neq 0$) carriers to be analyzed in magnetic field. However, from the model fits of reflectance to Eq. 2 one cannot determine which modes are electron- and which ones are hole-like. Kerr rotation spectroscopy measurements would be needed to distinguish between the two¹⁶. The reflectance

spectra were fit with the ReFFIT program¹⁷, in which Eq. 2 is implemented as one of the models.

We were able to fit all field curves, from 0 Tesla to 18 Tesla, with only two modes ($i = 1, 2$), one with positive and one with negative cyclotron frequency ($\omega_{c,1}$ and $\omega_{c,2}$ in Eq. 2). The results of the best fits at several selected field values are shown in Fig. 1(b) with gray lines. As can be seen, the fits with only two modes are able to capture the most important features of the data. At low fields the reflectance at low frequencies decreases, whereas above the plasma edge it increases: the plasma edge is gradually destroyed. At higher fields, characteristic new feature develops in reflectance which resembles another plasma edge (labeled mode γ in Fig. 1(b)), and it seems to harden with field. Indeed, as we will elaborate below, this feature is due to a new absorption channel, whose frequency increases with magnetic field.

In Fig. 2 we display the values of fitting parameters from Eq. 2 for all measured field values. We note that most parameters display discontinuity around 7 Tesla (marked with a dotted line in Fig. 2), which we interpret as the extreme quantum limit (EQL) in $\text{Bi}_{1-x}\text{Sb}_x$ at this doping level¹⁸. This value of the EQL is slightly lower than in pure Bi (9 Tesla)¹⁹, but higher than in $\text{Bi}_{1-x}\text{Sb}_x$ with $x = 0.04$ (3 Tesla)²⁰. Panel Fig. 2(a) displays the values of the two cyclotron frequencies $\omega_{c,1}$ and $\omega_{c,2}$. They have opposite signs, but for simplicity we show them both as positive in Fig. 2. In this particular fit, the mode $\omega_{c,1}$ was positive, and $\omega_{c,2}$ was negative. At lower fields, below the EQL, both $\omega_{c,1}$ and $\omega_{c,2}$ increase with field. Above the EQL they tend to saturate, or even decrease.

Figures 2(b) and (c) display the values of ω_0 , ω_p and γ for the two modes, respectively. These parameters show similar trends for both modes. The most dramatic change occurs for the ω_0 parameters, which are both zero below the EQL, but acquire finite values above EQL. Above 7 Tesla, both $\omega_{0,1}$ and $\omega_{0,2}$ increase with field. On the other hand, $\omega_{p,2}$ decreases significantly, especially above the EQL.

In order to get better insight into absorption processes in magnetic field we use the best fits obtained with Eq. 2 to generate model circular conductivities $\sigma_{\pm}(\omega) = \sigma_{xx} \pm i\sigma_{xy}$. They are related to the dielectric function tensor as¹⁵ $\sigma_{\pm}(\omega) = \omega(\epsilon_{\pm}(\omega) - 1)/(4\pi i)$. Fig. 3 displays real, dissipative parts of $\sigma_{\pm}(\omega)$. Low field curves, below EQL, are shown separately from the high field curves, for both $\sigma_+(\omega)$ and $\sigma_-(\omega)$. The top two panels (Fig. 3(a) and (b)) display low magnetic fields and as can be seen, both $\sigma_+(\omega)$ and $\sigma_-(\omega)$ are Drude-like at zero magnetic field. These Drude modes quickly shift to finite frequencies and harden as field increases. However, we note that the peak is at much higher frequencies in $\sigma_-(\omega)$ than in $\sigma_+(\omega)$ (note logarithmic frequency axis).

At higher fields (Fig. 3(c) and (d)), the system enters the EQL and charge dynamics becomes highly localized. Optical conductivity of both channels is dominated by strong Lorentzian peak, which shows little field depen-

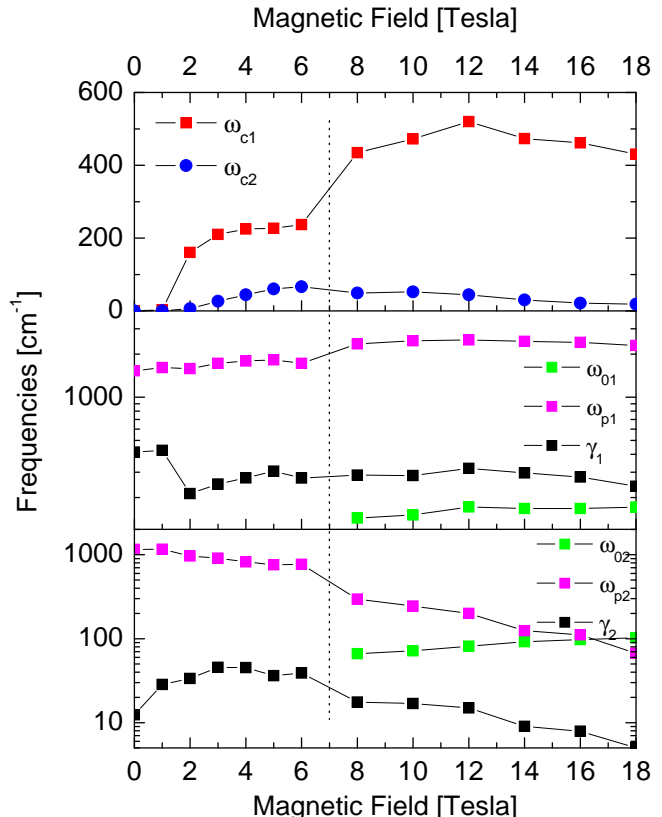


FIG. 2: (Color online). Fitting parameters for the fits shown in Fig. 1(b), as obtained from Eq. 2. Vertical dotted line represents the extreme quantum limit (EQL) discussed in the text. (a) Cyclotron frequencies of both modes. (b) Fitting parameters of the first mode. (c) Fitting parameters of the second mode.

dence. We again note that the peak is at much higher frequency in the $\sigma_-(\omega)$ component. In addition, another peak, superimposed on the main peak, is observed in both channels, and is at similar frequencies. These peaks appear to be due to Landau level (LL) transitions. The peak is at higher frequency in $\sigma_+(\omega)$ than in $\sigma_-(\omega)$, but in both $\sigma_+(\omega)$ and $\sigma_-(\omega)$ the peak is hardening, i.e. it shifts to higher frequencies as field increases. At the same time the intensity of both peaks gradually decrease as the field increases. In the inset of Fig. 3(c) we display field dependence of the central frequency of the peak ω_{LL} and the plot reveals that ω_{LL} of both peaks is approximately linear function of the field $\omega_{LL} \sim B$. Observed linear field dependence is to be contrasted with the $\omega_{LL} \sim \sqrt{B}$ behavior identified in $\text{Bi}_{1-x}\text{Sb}_x$ with $x = 0.09$ ²¹. Note however that for such high doping level, the system is already in the topological insulating regime. Our results should also be contrasted with the results on a canonical

topological insulator Bi_2Se_3 , where a single bulk and a single surface mode were found^{22,23}.

The two modes both display linear field dependence, however they display different behavior when extrapolated to zero field. Namely, the frequency of the peak in the σ_- channel extrapolates to zero, whereas the frequency of the peak in σ_+ extrapolates to a value of approximately 83 cm^{-1} (10 meV). The evolution of LL transitions in magnetic field has been discussed before²¹. Based on this discussion we conclude that LL modes observed in our study are due to bulk carriers, and that the one that extrapolates to zero frequency in zero field corresponds to inter-band LL transitions, whereas the one that extrapolates to finite value corresponds to intra-band LL transitions.

IV. SUMMARY

In summary, we have presented magneto-optical data for $\text{Bi}_{1-x}\text{Sb}_x$ in magnetic fields up to 18 Tesla. As the field increases the optical functions are altered, indicating strong sensitivity of charge carriers to external magnetic field. Our analysis indicates that two types of charge carriers are present, and they respond similarly to field. Above 7 Tesla, in the extreme quantum regime, the response of the system is quite localized, as indicated by a strong Lorentz-like peak in the optical conductivity. In addition, we observe absorption features that are most likely due to Landau level transitions, both inter- and intra-band. Finally, our data reveals similarities, but also some important differences compared with pure Bi. More notably, the two modes (α and β) present in pure Bi, are absent from the spectra of $\text{Bi}_{1-x}\text{Sb}_x$. The other two modes (γ and δ) are present in both systems and follow similar field evolution.

The authors thank A.D. LaForge and A.A. Schafgans for useful discussions. S.V.D. acknowledges the support from The University of Akron FRG. Magneto-optical measurements were carried out at the National High Magnetic Field Laboratory, which is supported by NSF Cooperative Agreement No. DMR-0654118, by the State of Florida, and by the DOE.

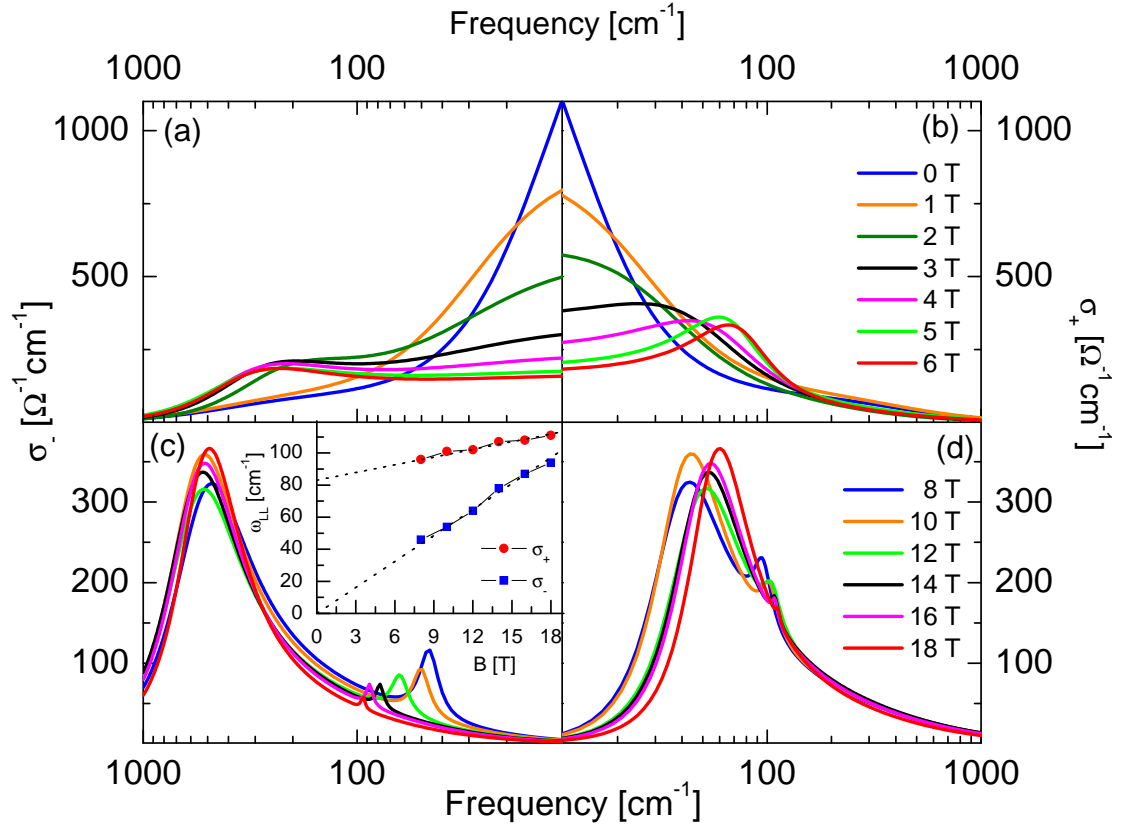


FIG. 3: (Color online). Real part of σ_- ((panels (a) and (c))) and σ_+ ((panels (b) and (d))) calculated from the best fits of reflectance using Eq. 2. Low magnetic fields below 7 Tesla (panels (a) and (b)) are shown separately from high magnetic fields above 7 Tesla (panels (c) and (d)). The inset displays the field dependence of the two peaks. Both peaks follow linear dependence, however for one of them the extrapolated value is finite, whereas for the other it is zero.

-
- * Electronic address: dsasa@uakron.edu
- ¹ M.Z. Hasan and C.L. Kane, *Reviews of Modern Physics* **82**, 3045 (2010).
 - ² Xiao-Liang Qi and Shou-Cheng Zhang, *Reviews of Modern Physics* **83**, 1057 (2011).
 - ³ D. Hsieh, D. Qian, L. Wray, Y. Xia, Y. S. Hor, R. J. Cava and M.Z. Hasan, *Nature* **452**, 970 (2008).
 - ⁴ D. Hsieh, Y. Xia, L. Wray, D. Qian, A. Pal, J.H. Dil, J. Osterwalder, F. Meier, G. Bihlmayer, C.L. Kane, Y.S. Hor, R.J. Cava and M.Z. Hasan, *Science* **323**, 919 (2009).
 - ⁵ P. Roushan, J. Seo, C.V. Parker, Y.S. Hor, D. Hsieh, D. Qian, A. Richardella, M.Z. Hasan, R.J. Cava and A. Yazdani, *Nature* **460**, 1106 (2009).
 - ⁶ M. Dressel and G. Gruner, *Electrodynamics of Solids*, Cambridge University Press, Cambridge (2001).
 - ⁷ D.N. Basov and T. Timusk, *Reviews of Modern Physics* **77**, 721 (2005).
 - ⁸ S.V. Dordevic and D.N. Basov, *Annalen der Physik* **15**, 545 (2006).
 - ⁹ P.M. Nikolic, S.S. Vujatovic, T. Ivetic, M.V. Nikolic, O. Cvetkovic, O.S. Aleksic, V. Blagojevic, G. Brankovic, N. Nikolic, *Science of Sintering* **42**, 45 (2010).
 - ¹⁰ C.C. Homes, M.A. Reedyk, D.A. Crandles and T. Timusk, *Applied Optics* **32**, 2976 (1993).
 - ¹¹ S.V. Dordevic, Seiki Komiya, Yoichi Ando, Y.J. Wang and D.N. Basov, *Physical Review B* **71**, 054503 (2005).
 - ¹² V.S. Edelman, *Advances in Physics* **25**, 555 (1976).
 - ¹³ A.D. LaForge, A. Koncz, A. Kuzmenko, T. Lin, X. Liu, J. Shi, S.V. Dordevic and D.N. Basov, <http://meetings.aps.org/link/BAPS.2010.MAR.H15.4>
 - ¹⁴ R. Tediosi, N. P. Armitage, E. Giannini and D. van der Marel, *Physical Review Letters* **99**, 016406 (2007).
 - ¹⁵ B. Lax and J.G. Mavroides, in *Semiconductors and Semimetals*, edited by R.K. Willardson and A.C. Beer, Academic Press, New York and London (1967).
 - ¹⁶ J. Levallois, M.K. Tran, A.B. Kuzmenko, arXiv:1110.2754.
 - ¹⁷ A.B. Kuzmenko, *Reviews of Scientific Instruments* **76**, 083108 (2005).
 - ¹⁸ In the extreme quantum limit (EQL) all charge carriers are in the lowest Landau Level.
 - ¹⁹ K. Behnia, L. Balicas and Y. Kopelevich, *Science* **317**, 1729 (2007).
 - ²⁰ A. Banerjee, B. Fauque, K. Izawa, A. Miyake, I. Sheikin, J. Flouquet, B. Lenoir and K. Behnia, *Physical Review B* **78**, 161103(R) (2008).
 - ²¹ A.A. Schafgans, A.A. Taskin, Yoichi Ando, Xiao-Liang Qi, B.C. Chapler, K.W. Post, D.N. Basov, arXiv:1202.4029.
 - ²² A.B. Sushkov, G.S. Jenkins, D.C. Schmadel, N.P. Butch, J. Paglione and H.D. Drew, *Physical Review B* **82**, 125110 (2010).
 - ²³ G.S. Jenkins, A.B. Sushkov, D.C. Schmadel, N.P. Butch, P. Syers, J. Paglione and H.D. Drew, *Physical Review B* **82**, 125120 (2010).